Letters in Applied NanoBioScience
Open-Access Journal (ISSN: 2284-6808)

Article
Volume 13, Issue 2, 2024, 97
https://doi.org/10.33263/LIANBS132.097

Activities of Analogues of Carbamazepine and (R)–Lacosamide as Potential Inhibitors of Epilepsy Disease: Molecular Docking, DFT, and Pharmacokinetic Study

Isaiah A. Adejoro [1], Damilare D. Babatunde [1,2,*], Okegbemi Z. Folashade [1], Hikmat A. Olayiwola [1], Chinonyerem A. G. Johnson [1], Amaka D. Ikechukwu [1]

[1] Department of Chemistry, Faculty of Science, University of Ibadan, Ibadan, Nigeria
[2] Department of Chemistry, College of Science, Engineering and Technology, University of South Africa, Florida, Johannesburg 1709, South Africa
* Correspondence: damilarebabatunde21@gmail.com;

Scopus Author ID 57939606900
Received: 14.05.2023; Accepted: 22.01.2024; Published: 30.06.2024

Abstract: The increasing incidence of resistance to current epilepsy therapy underscores the need to develop new antiepileptic agents with a new mechanism of action. Lacosamide and Carbamazepine derivatives structurally related to the antiepileptic drugs were reported to be devoid of Carbonic anhydrase inhibitory properties. Computational modeling can be a powerful tool for an experimentalist, providing rigorous algorithms for the system of study. This can be valuable in testing hypotheses and developing experimental protocols before experimenting. Therefore, this study aims to use computational methods to confirm the experimental claim of the selected epilepsy inhibitors. Through the hybrid functional B3LYP 6-311++G (d,p) associated with ADME/Tox (absorption, distribution, metabolism, excretion, and Toxicity) predictions, the drug-ability, the physicochemical, pharmacodynamic, and pharmacokinetic properties of the analogs as potential inhibitors were investigated. All the compounds passed Lipinski's rule of five, indicating their potential oral use. To understand the mode of interaction and the binding energy, molecular docking studies of the analogs have been carried out with multiple targets such as Voltage-gated T-type calcium channel ($Ca_v3.1$), Voltage-gated sodium channel alpha ($Na_v1.5$), human Carbonic Anhydrase 2 (hCA-II), and γ-amino butyric acid receptor ($GABA_B$). The compounds of BIA 2-024, Carbamazepine, and Eslicarbazepine showed the best docking interactions and ΔG° results when docked with most of the receptors. These results predict the role of these compounds as potential antiepileptic drugs (AEDs).

Keywords: epilepsy; anticonvulsant activity; antiepileptic drugs; Lacosamide; Carbamazepine; molecular docking; DFT; ADMET; sodium channel; calcium channel; carbonic anhydrase.

1. Introduction

Ion influx through neuronal voltage-dependent ion channels mediates a range of cytoplasmic responses, including releasing neurotransmitters, activating Ca^{2+}-dependent enzymes, and controlling neuronal excitability. Voltage-gated calcium channels are important brain, heart, and muscle function regulators. An epileptic seizure is a brief period of symptoms resulting from unusually intense or coordinated neural activities in the brain. Epilepsy is a brain illness defined by a lasting proclivity to produce epileptic seizures as well as the neurobiological, cognitive, psychological, and social implications of this condition [1,2]. These episodes can also occur with subtle or no behavioral signs. Epilepsy is one of the numerous

pathophysiological conditions connected to excessive Ca^{2+} entry into the cytosol, as well as mutations and deletions in genes encoding Ca^{2+} channels; others include migraine, pain, autism, cerebellar ataxia, and night blindness [3,4]. The devastating neurodegenerative disorder has no lasting potent disease-modifying therapy currently available. There is presently no long-term effective disease-modifying medication available for this terrible neurological condition.

Many therapeutic targets have been proposed, including Voltage-gated T-type calcium channel ($Ca_v3.1$) [3], Voltage-gated sodium channel alpha $Na_v1.5$, human Carbonic Anhydrase 2 (hCA-II), and γ-amino butyric acid receptor ($GABA_B$), which causes this disease. However, treatment regimens comprising combinations of these agents have significantly reduced the activity of epilepsy. Voltage-gated ion channels (VGICs), which are widely distributed throughout the central nervous system (CNS), are responsible for the creation and control of neuron excitability and are considered important actors in the etiology of human epilepsy, regulating the form and duration of action potentials (APs).

The central nervous system (CNS) relies on various kinds of calcium (Ca^{2+}) channels, with T-type channels being one of the distinct types that play a crucial role in physiological functions [5]. These channels activate when the potential exceeds *–40 mV*, exhibit a small unitary conductance, and inactivate quickly upon opening [3]. In a Ca^{2+}-dependent manner, Ca^{2+} channels physically bind to proteins of the vesicle-release machinery, which can influence their activity [6]. In some cases, knowledge about how drugs interact with other ion channels, such as sodium channels, has been used to identify drug interaction sites on voltage-gated calcium channels, including T-type channels. In T-type channels, the *S6* regions in domains III and IV of the *Cavα1* subunit are hotspot locations for drug interaction sites. These regions are linked to the inactivation-gating machinery and are located within the inner vestibule of the channel pore [4]. Modulation of Ca^{2+} channels occurs through different mechanisms, including control by G-proteins and second messengers [7]. One highly versatile and widely expressed Ca^{2+} sensor, calmodulin (CAM), regulates the function of many enzymes and ion channels. The voltage-gated Ca^{2+} channels $Ca_v1.2$ (Ca^{2+}-dependent inactivation) and $Ca_v2.1$ (Ca^{2+}-dependent facilitation) are both subject to regulation by CAM, with CAM interacting with Ca^{2+}-bound channels to produce Ca^{2+}-dependent inactivation and facilitation [8]. Calcium channel blockers have proven effective in treating absence seizures and are becoming increasingly recognized as potential therapeutic pathways for a variety of disorders, including pain, Parkinson's disease, addiction, and anxiety. As a result, Ca^{2+} channels are critical pharmaceutical targets, and a thorough understanding of the processes that regulate their activity is essential.

As of 2022, approximately 50 million people worldwide have epilepsy, with nearly 80% of cases occurring in developing countries [9]. In 2015, epilepsy was responsible for 125,000 deaths, an increase from 112,000 in 1990 [10]. Currently, drugs remain the primary treatment for epilepsy. Over 35% of available antiepileptic drugs target voltage-gated ion channels (VGICs), including phenytoin, gabapentin, Carbamazepine, Oxcarbazepine, and ethosuximide. Phenytoin and Carbamazepine (CBZ) are broad-spectrum antiepileptic drugs that primarily function by blocking voltage-gated sodium channels (VGSCs). Phenytoin, for example, is more effective at inhibiting SCN8A-I1327V than other drugs and could be used to treat patients with gain-of-function mutations of SCN8A [11]. Different types of VGICs are involved in the pathological process of epilepsy in distinct ways. For example, a decrease in the expression of P/Q type VGICs may lead to the development of epilepsy. At the same time, an increase in the expression of N-type and T-type calcium channels could also contribute to

epileptic activity. These variants are essential for the disorder's prognosis and medication outcomes [12]. These findings suggest that the regulation of VGICs could be a potential therapeutic target for managing epilepsy [13].

CBZ is a first-line drug and also an oral sodium channel blocker approved for the treatment of seizures and neuropathic pain. However, CBZ is a drug that is effective in reducing pain levels. Still, it comes with a variety of therapy-limiting side effects, such as fatigue, elevated liver enzymes, and diarrhea, as well as a lack of pain improvement, which led to CBZ discontinuation [14]. Meanwhile, a study on stress degradation by Ghosh M et al. shows that oxidation and acid degradation mostly impact CBZ solutions [15]. Various derivatives of CBZ have been examined to have more anticonvulsant efficacy over CBZ-resistant seizures [16,17].

Lacosamide (LCM) is a third-generation antiepileptic drug (AED) that possesses a favorable pharmacokinetic and pharmacodynamic profile that has been approved as an adjuvant treatment for difficult-to-control partial seizures, with or without subsequent generalization [18]. Its primary use is as an adjuvant treatment for refractory partial seizures. It has a dual mechanism of action that includes the inactivation of slow Na^+ channels and modulation of response to type 2 collapsin [19]. LCM treatment has been found to be effective for treating epilepsy in Japanese pediatric patients, particularly at higher doses. The level of LCM in the patient's blood may have a stronger relationship with its effectiveness than the actual dosage administered [20]. A multivariate analysis of LCM treatment revealed that patients who underwent gross-total resection at the time of diagnosis had a significantly higher chance of seizure-free after 6 months. The side effects of LCM treatment were generally mild, and only a small number of patients (about 1.5%) discontinued treatment. The most commonly reported side effects were dizziness and sleepiness [21]. Another study findings by Çarçak et al. suggest that long-term LCM treatment may modify the development of absence seizures in GAERS and positively affect absence seizure epileptogenesis [22]. The antiepileptic drug (R)-lacosamide (R-LCM), ((R)-2-acetamido-N-benzyl-3-methoxypropanamide) and its derivatives were efficiently and scalable synthesized from commercially existing aziridine-(2R)-carboxylate in three simple sequential steps, including regioselective aziridine ring opening, debenzylation followed by acetylation in one pot, and amide formation [23]. The derivatives of R-LCM are (R)-2-acetamido-N-benzyl-3-ethoxypropanamide (**1a**), (R)-2-acetamido-N-benzyl-3-propoxypropanamide (**1b**), (2R)-2-acetamido-N-(((1R,3S,5R)-adamantane-2-yl)methyl)-3-methoxypropanamide (**1c**), (R)-2-acetamido-N-cyclopentyl-3-methoxypropanamide (**1d**), (R)-2-acetamido-N-hexyl-3-methoxypropanamide (**1e**), (R)-2-acetamido-N-decyl-3-methoxypropanamide (**1f**), (R)-2-acetamido-N-dodecyl-3-methoxypropanamide (**1g**), and (R)-2-acetamido-N-octadecyl-3-methoxypropanamide (**1h**) (Figure 1). Meanwhile, the derivatives CBZ are 10-oxo-10,11-dihydro-5H-dibenzo[b,f]azepine-5-carboxamide (**OXC**), (S)-10-hydroxy-10,11-dihydro-5H-dibenzo[b,f]azepine-5-carboxamide (**Eslicarbazepine**), (S)-(-)-10-acetoxy- 10,11-dihydro-5H-dibenz[b,f]azepine-5-carboxamide (**BIA 2-093**), and (Z)-10-(hydroxyimino)-10,11-dihydro-5H-dibenzo[b,f]azepine-5-carboxamide (**BIA 2-024**) (Figure 2).

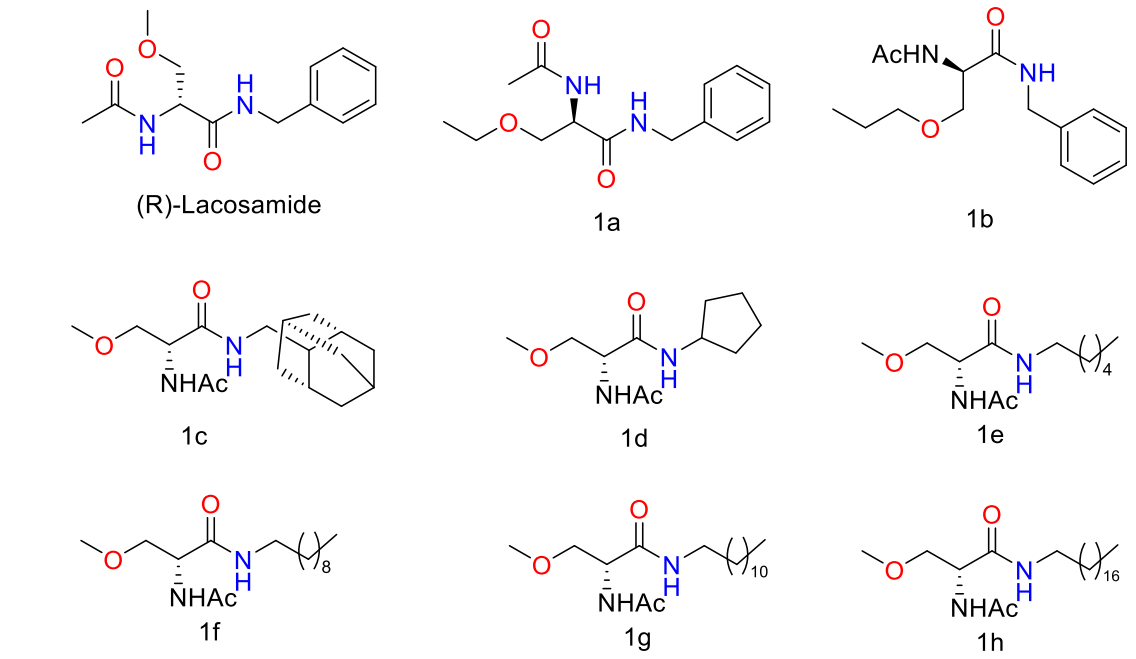

Figure 1. Structural formulae of R-LCM and its synthesized analogs.

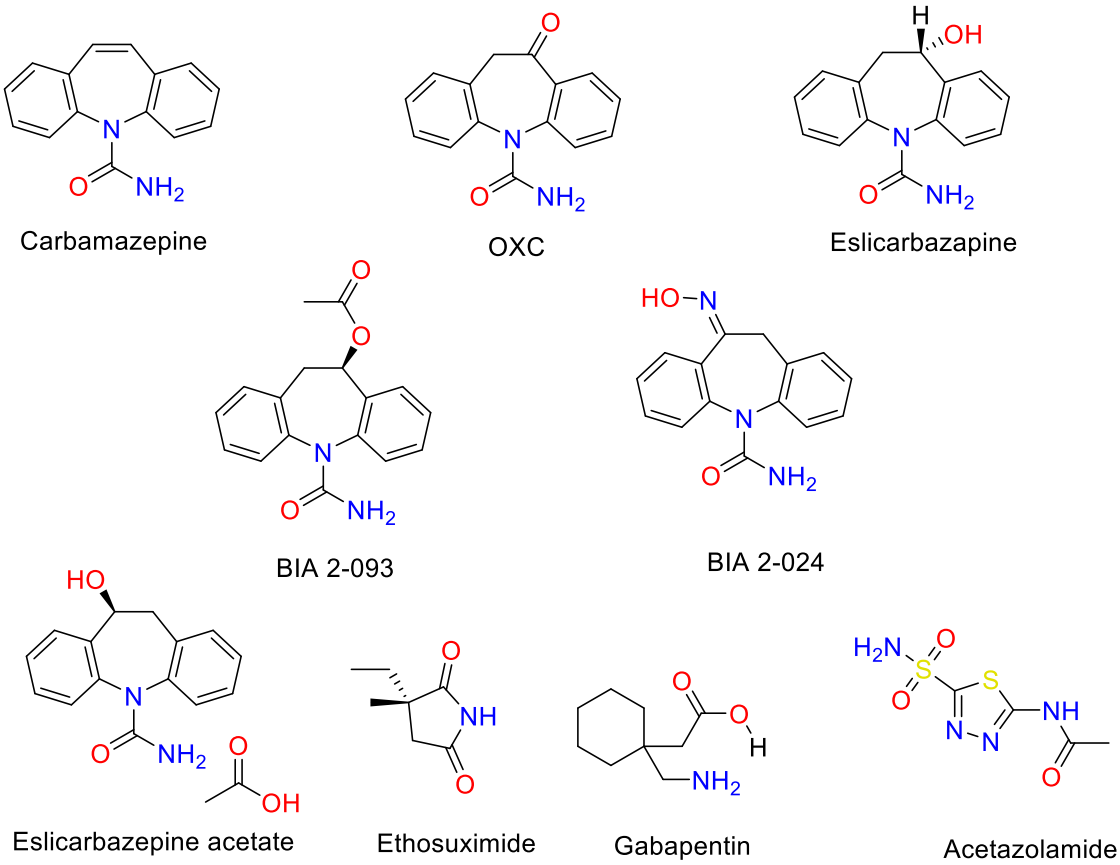

Figure 2. Structural formulae of CBZ and its analogues; (oxcarbazepine (OXC), Eslicarbazepine, BIA 2-093, and BIA 2-024). The last four compounds (Ethosuximide, Gabapentin, Acetazolamide, and Eslicarbazepine acetate) are the structural formulae of the FDA-approved drugs and the standards used in this study.

Consequently, this research aims to investigate the inactivation activity of the existing synthesized R-LCM and CBZ derivatives in complex reactions with different receptors responsible for epilepsy. Thereby further modeling new materials that can improve the efficiency of the existing drugs [23,24]. If one compound cannot inhibit the different targets,

we aim to consider the different targets they can inhibit and how to develop this into better AEDs.

2. Materials and Methods

This study was designed to examine the interactions of the analogs of R-LCM and CBZ in complex with the major targets of epilepsy. We did drug-likeness scoring, ADMET profile study, and Protein-ligand docking to evaluate the lead potency of the compounds. The analogs' binding modes and stability are compared to the FDA-approved drugs.

2.1. Macromolecule preparation.

The X-ray crystal structure of the proteins complexed with their co-crystallized ligands was obtained from the Protein Data Bank [25]. γ-amino butyric acid receptor ($GABA_B$; 4MS3, Resolution: 2.50 Å) [26], Voltage-gated T-type calcium channel ($Ca_v3.1$; 6KZO, Resolution: 3.30 Å) [27], Voltage-gated sodium channel alpha ($Na_v1.5$; 4OVN, 6MUD, Resolution: 2.80 Å, 2.69 Å respectively) [28,29], and human Carbonic Anhydrase 2 (hCA-II; 5FDC, Resolution: 1.75 Å) [30]. The target proteins were stripped of all crystal water molecules and heteroatoms. We used Computed Atlas for Surface Topology of Proteins (CASTp) [31] to define the binding sites of the target receptors. The obtained amino acid residues of the binding sites were further validated using the reported experimental binding pockets for the target proteins using X-ray crystallography. The docking procedure has been evaluated by re-docking the native co-ligands in the active sites of the receptors.

2.2. Quantum chemical calculations.

From the literature, we selected a series of synthesized compounds of R-LCM and Carbamazepine analogs, which were reported as potential anticonvulsant compounds [23,32]. The compound's 3D molecular structures were energetically minimized and geometrically optimized in their most conforming ground state using density functional theory (DFT) with Becke, 3-parameter, Lee–Yang–Parr (B3LYP) method with a basis set 6-311++G (d,p) [33,34] calculations using Spartan '14 version 1.1.4. After optimization, the molecular structures were saved as PDB files.

2.3. Drug Likeness and ADME/Tox profile.

Using MolSoft [35], the drug-likeness score (≥ 0.18) of each ligand was determined using Lipinski's criteria [36]. To maximize the discovery of the fully active compounds, the following probability parameters were predicted using admetSAR2.0 [37]: the human intestinal absorption (HIA), caco-2, human oral bioavailability (≥ 30%), blood-brain barrier permeability, P-glycoprotein, CYP2D6, CYP2C9, CYP3A4, and CYP1A2 inhibition, eye irritation, Ames mutagenesis, human ether-a-go-go inhibition, and hepatotoxicity. These parameters are used to analyze the pharmacokinetics of the compounds, which are the most important indicators for evaluating the characteristics of ADME/Tox (absorption, distribution, metabolism, excretion, and Toxicity) predictions.

2.4. Molecular docking.

BIOVIA Discovery Studio was used to prepare the imported protein structure, then the required amounts of hydrogen atoms were added, and the structure was refined. The water molecules in the crystallographic complex were eliminated from the crystal structure, and the repeat protein chains were removed from the crystal structure. A molecular docking method used in our previous studies [38] was applied in this work. AutoDock Vina incorporated in PyRx [39] was used for the molecular docking. The docking protocol was run three times with different random seeds. The binding modes were clustered and analyzed visually in Discovery Studio.

More so, molecular interactions between the studied analogs of R-LCM and CBZ complex with the targets were studied by observing the binding affinity for each compound, the residues involved in the interaction, and the type of non-bonding interaction that occurs between the complexes. The study of the mechanism of action of CBZ and its derivatives developed by BIAL [32], Oxcarbazepine (OXC), (S)-(-)-10-acetoxy-10,11-dihydro-5H-dibenz[b,f]azepine-5-carboxamide (BIA 2-093) and 10,11-dihydro-10-hydroxyimino-5H-dibenz[b,f]azepine-5-carboxamide (BIA 2-024) was reported. The experimental data indicated that the primary reason for the effectiveness of these antiepileptic drugs (AEDs) in preventing seizure is the suppression of sodium channel activity.

3. Results and Discussion

3.1. Density functional theory analysis.

In this study, density functional theory (DFT) using the B3LYP/6- 311++G (d,p) basis set was used to derive the optimal molecular geometries of the compounds together with their atomic numbering schemes. The optimized structures at their ground state yielded calculated parameters: octanol-water partition coefficient (log P), dipole moment, ovality, polarizability, the number of hydrogen bond donors (HBDs) and acceptors (HBAs) and acceptor sites (HBAs), area, volume, polar surface area (PSA), the lowest unoccupied molecular orbital (ε_L), the highest occupied molecular orbital (ε_H) (Table 1). The reactive behavior parameters for the most stable conformers were derived from the other quantum chemical parameters (equations 1 – 5) and are listed in Table 2. The derived quantum chemical parameters are given the following simple expressions [40,41]:

$$\Delta E = \varepsilon_L - \varepsilon_H \quad (1)$$

$$\mu \approx \frac{\varepsilon_H + \varepsilon_L}{2} \quad (2)$$

$$\chi = -\mu \quad (3)$$

$$\eta \approx \varepsilon_L - \varepsilon_H \quad (4)$$

$$\omega = \frac{\mu^2}{2\eta} = \frac{\mu^2}{2}\sigma \quad (5)$$

Table 1. Predicted molecular properties (using DFT, B3LYP/6-311++G (d,p)) of the potential inhibitor candidates in a vacuum from equilibrium geometry at the ground state.

Name	E (au)	ε_H (eV)	ε_L (eV)	CPK Area (Å^2)	CPK Volume (Å^3)	PSA (Å^2)	CPK Ovality	Log P	Polarizability	HBD Count	HBA Count
1a	-448.41	-9.76	0.07	321.89	286.45	58.203	1.53	0.20	62.29	2	5
1b	-920.04	-6.40	-0.56	339.04	304.18	54.325	1.55	-0.11	64.67	2	5

Name	E (au)	ε_H (eV)	ε_L (eV)	CPK Area (Å^2)	CPK Volume (Å^3)	PSA (Å^2)	CPK Ovality	Log P	Polarizability	HBD Count	HBA Count
1c	-999.88	-6.46	0.47	345.62	327.57	53.171	1.50	0.43	66.31	2	5
1d	-766.40	-6.41	0.33	276.72	245.19	54.734	1.46	-0.74	59.67	2	5
1e	-806.93	-6.43	0.32	316.29	275.33	55.336	1.55	0.20	62.11	2	5
1f	-964.18	-6.52	0.43	398.13	349.4	53.903	1.66	1.87	68.07	2	5
1g	-1042.81	-6.48	0.49	435.83	385.88	54.296	1.70	2.71	71.03	2	5
1h	-1278.69	-6.50	0.46	555	496.43	54.433	1.83	5.21	80.00	2	5
(R) LCM	-841.42	-6.38	-0.02	295.04	266.7	48.018	1.47	-0.14	61.50	2	5
CBZ	-763.59	-5.78	-1.36	254.13	245.78	36.871	1.34	-0.32	60.27	1	3
OXC	-838.82	-6.30	-1.55	260.21	252.38	50.333	1.35	-0.60	60.72	1	4
BIA 2-024	-894.12	-5.91	-1.04	273.75	263.82	66.97	1.38	-0.21	61.62	2	5
BIA 2-093	-992.68	-6.06	-0.73	309.12	298.23	55.201	1.43	-0.86	64.31	1	4

Table 2. Calculated quantum parameters (using DFT, B3LYP/6-311++G (d,p)) of the potential inhibitor candidates.

	ΔE (eV)	I (eV)	A (eV)	η (eV)	χ (eV)	σ (eV)	μ (eV)	ω (eV)
(R) LCM	6.36	6.38	0.02	6.36	3.20	0.16	-3.20	0.805
1a	9.83	9.76	-0.07	9.83	4.85	0.10	-4.85	1.196
1b	5.84	6.40	0.56	5.84	3.48	0.17	-3.48	1.037
1c	6.93	6.46	-0.47	6.93	3.00	0.14	-3.00	0.649
1d	6.74	6.41	-0.33	6.74	3.04	0.15	-3.04	0.685
1e	6.75	6.43	-0.32	6.75	3.06	0.15	-3.06	0.694
1f	6.95	6.52	-0.43	6.95	3.05	0.14	-3.05	0.669
1g	6.97	6.48	-0.49	6.97	3.00	0.14	-3.00	0.646
1h	6.96	6.50	-0.46	6.96	3.02	0.14	-3.02	0.655
BIA 2-024	4.87	5.91	1.04	4.87	3.48	0.21	-3.48	1.243
BIA 2-093	5.33	6.06	0.73	5.33	3.40	0.19	-3.40	1.084
CBZ	4.42	5.78	1.36	4.42	3.57	0.23	-3.57	1.442
OXC	5.75	6.30	1.55	5.75	3.93	0.17	-3.93	1.343

ΔE – energy gap, χ – electronegativity, I – ionization potential, A – electron affinity, μ – chemical potential, η – chemical hardness, σ – chemical softness, and ω – global electrophilicity index

The energy gap (ΔE) between the LUMO and HOMO influences the reactivity of the inhibitor molecules greatly. Inhibitor molecule with low ΔE values gives better inhibition properties because little energy is needed to remove an electron from the last occupied molecular orbital [42]. According to the values of the energy gap, ΔE, from Table 2, it reveals that Carbamazepine, BIA 2-024, BIA 2-093, and Eslicarbazepine acetate showed the lowest ΔE compared with the other compounds, which suggests high chemical reactivity and considerable intramolecular charge transfer from an electron donor (HOMO) to electron acceptor (LUMO) groups. Based on these results, Carbamazepine, BIA 2-024, and BIA 2-093 have better bioactivity than the other studied compounds by considering the energy gap (ΔE). Global softness, σ, demonstrates the molecule's susceptibility to charge transfer. Carbamazepine, BIA 2-024, BIA 2-093, Oxcarbazepine, and 1b are the first five compounds with the **σ** value (0.23 eV, 0.21eV, 0.19eV, 0.17eV, and 0.17eV respectively) in a vacuum. These compounds are the softest molecules, the most susceptible to charge transfer, and the most chemically reactive. The charge of the chemical species is also associated with resistance to electron transfer in the molecule; this defines the system's chemical hardness. Some of the R-LCM derivatives (1a, 1c, 1f, 1g, and 1h) have the highest chemical hardness compared to other compounds, making them more resistant to electron transfer. The global electrophilicity index, ω, measures the stability of the energy of the system when it acquires an additional

electronic charge N from the environment (Eq. 5). The electrophilicity scale is a simple way to assess the polarity of an interaction based on the electrophilicity gap between the reacting partners [41]. A comparison between the calculated global electrophilicity indexes of the compounds revealed the reactivity nature and stability of the individual compounds. The expected charge transfer from the calculated ω reveals that CBZ > Oxcarbazepine > BIA 2-024 > 1a > BIA 2-093 and so on. Electronegativity, χ, is a measure of electron distribution in the molecule [43]. The high electronegativity obtained for these compounds indicates they are good electron acceptors. Compound 1a had the highest χ value (4.85 eV), while compounds 1c and 1g had the lowest (3.00 eV) (Table 2). The chemical potential (μ) signifies the (μ) signifies the likelihood of a chemical reaction. A higher μ value implies a greater ease of electron donation (as an electron donor). Conversely, a lower μ value (more negative) indicates a higher propensity to accept electrons (as an electron acceptor) [44]. Most of the compounds exhibit the ability to engage in a chemical reaction as electron donors.

3.2. ADME and toxicity analysis.

Table 2 shows the results of the Lipinski rule of five analyses on the fifteen lead compounds. All the compounds passed the rule of five with zero violations except compound 1h, which has one violation. Table 3 shows the possible adsorption and toxicity profiles of the fourteen candidate compounds as predicted by the admetSAR server, while Table 4 shows the distribution profile of the compounds as predicted by the admetSAR server. Any molecule involved in the central nervous system (CNS) drug development project has to be an optimal candidate capable of crossing the blood-brain barrier (BBB) [45,46]. The BBB separates circulating blood and cerebrospinal fluid (CSF) in the CNS. It consists of endothelial cell-formed tight junctions surrounding capillaries that specifically block the diffusion of microscopic particles and big or hydrophilic molecules into the CSF while allowing the passage of tiny hydrophobic molecules. Specific proteins with other metabolic products, such as glucose, are actively transported over barriers by barrier cells. Carbamazepine, Oxcarbazepine, Eslicarbazepine, BIA 2-024, and BIA 2-093 have the highest blood-brain permeability. This is an assessment that all the studied compounds can pass the blood-brain barrier, implying they have good drug-like properties.

3.3. Molecular docking and binding domain interactions.

Docking was validated by re-docking the native ligands from crystal structures of receptors obtained from the RCSB Protein Data Bank. The assessment of the docking process's quality involves employing the lowest Root Mean Square Deviation (RMSD), which corresponds to the least binding energy, in order to evaluate the accuracy of replicating the binding pose of the molecular complex. The co-ligands associated with 4MS3 (γ-amino-butanoic acid) and 5FDC (3-[(sulfamoyl amino)methyl]-1-benzothiophene) exhibit respective ΔG values of -2.5 and -6.4 kcal/mol with their corresponding receptors. The interactions between the co-ligand of 5FDC and the receptor are illustrated in Figure 3, both prior to (A) and post-docking (B). The outcome of the docking validation shows a consistent alignment between docking poses and their atomic interactions. This underscores the capability of the docking protocol to accurately reproduce analogous docking poses of the ligand about its original crystal-bound conformation [47]. Consequently, the efficacy of the docking protocol is affirmed.

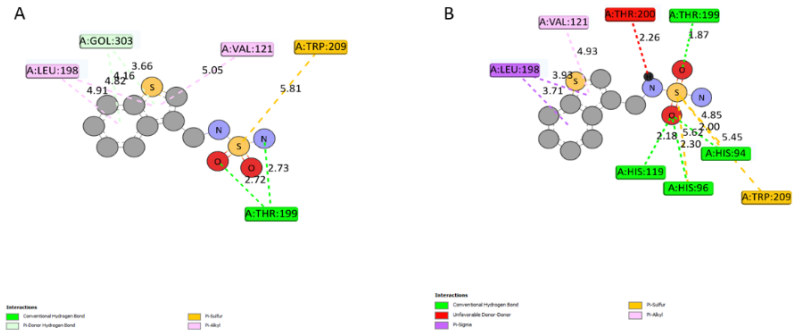

Figure 3. The X-ray crystallographic ligand-receptor complex (A) and the docked ligand in its originally bound-receptor complex (B) of the hCA-II (5FDC) receptor.

Our current efforts to identify novel anti-epilepsy agents focus on searching for inhibitors of $Ca_v3.1$, $Na_v1.5$, hCA-II, and $GABA_B$. The molecular docking results of the protein-ligand complexes were evaluated according to their binding interactions and the calculated binding free energy results, as exhibited in Table 3. Six and nine out of the total studied nineteen compounds had a better binding affinity ($\Delta G \leq -5.9, -6.1$) in complex with $Na_v1.5$ (6MUD and 4OVN respectively) than the chosen standards (i.e., Ethosuximide, Acetazolamide, and Gabapentin); these compounds are BIA-2024, Eslicarbazepine, Carbamazepine, BIA-2093, Oxcarbamazepine, compounds 1a, 1b, 1c, and R-LCM.

Table 3. Calculated binding free energies.

Ligand	6KZO	6MUD	4OVN	5FDC	4MS3	Total
	$Ca_v3.1$	$Na_v1.5$		hCA-II	$GABA_B$	
1a	**-6.6**	-5.4	**-6.3**	**-7.4**	-6.2	**-31.9**
1b	-5.9	-5.3	**-6.3**	**-6.7**	-6.2	**-30.4**
1c	**-7.7**	**-5.9**	**-6.7**	-6.4	**-6.9**	**-33.6**
1d	-5.5	-4.6	-5.2	-5.9	-5.4	**-26.6**
1e	-5.5	-4.6	-5.3	-5.9	-4.8	**-21.3**
1f	-5.4	-4.4	-5.1	-5.5	-5.2	**-25.6**
1g	-4.7	-4.5	-5.2	-5.3	-5.4	**-25.1**
1h	-6.5	-4.4	-4.6	-5.3	-5.2	**-26**
Acetazolamide	-5.8	-5	-5.8	-6.4	-6.3	**-29.3**
BIA 2-024	**-8.0**	**-7.6**	**-7.3**	**-7.5**	**-8.1**	**-38.5**
BIA 2-093	**-8.0**	**-6.6**	**-7.2**	**-7.8**	**-7.6**	**-37.2**
Carbamazepine	**-8.1**	**-7.0**	**-7.4**	**-8.4**	**-7.8**	**-38.7**
Eslicarbazepine	**-7.8**	**-7.1**	**-7.2**	**-8.3**	**-7.6**	**-38**
Ethosuximide	-5.2	**-5.9**	-5.3	-5.1	-5.2	**-26.7**
Gabapentin	-5.0	-4.6	-5.5	-5.2	-5.3	**-25.6**
(R)-LCM	**-5.9**	-5.5	-6.1	**-7.0**	**-6.4**	**-30.5**
Oxcarbazepine	**-7.9**	**-6.6**	**-7.0**	**-8.0**	**-7.6**	**-37.1**

Direct binding evaluation provides additional information about drug interactions with the cytoplasmic membranes. First, the docked compounds' binding energy ($\Delta G°$) was compared with the results of the docked standard drugs. Then, the molecular interaction of compounds was visualized using the reported catalytic residues from the downloaded proteins. In $Na_v1.5$ (6MUD) target interactions, BIA 2-024 has the highest hydrogen bond interactions with residues ARG 106, HIS 107, VAL 108, MET 109, THR 110, GLY 113, LYS 115, and SER I:1904 with the distance 2.73, 2.79, 2.65, 2.44, 2.36, 2.16, 2.08, and 2.74 Å respectively, (Figure 4). These residues are located in the C-lobe of the IQ domain. The visualization result revealed that the top three compounds bonded with the IQ domain of the protein (Figure 4). Meanwhile, comparing this result with the 4ONV macromolecule, BIA-2-024, which has the

best binding energy bonded to the Brugada mutation (SER 1904) at the boundary of CTNa$_v$1.5 with the CaM-C-term lobe environment [28]. Brugada Mutations signal a genetic condition that causes an irregular heartbeat (ventricular fibrillation), causing the heart not to pump enough blood to the rest of the body. Brugada Syndrome causes this mutation. To assess this risk, genetic testing is performed to check for a mutation in the SCN5A gene. Meanwhile, carbamazepine's OH group interacted with the Brugada mutation residue (ARG 1914) of the protein structure 4NOV with a distance of 2.75 Å. In addition, The Amide and OH groups on CBZ form a hydrogen bond interaction with the mutation in the αI helix of the EF-hand-like motif (GLU 1799) of the Na$_v$1.5 (4NOV) with 2.75 Å. This results in the shift of the steady-state inactivation ($V_{0.5}$) in the hyperpolarizing direction, resulting in slow recovery from inactivation. Table 4 summarizes the interaction of all the compounds with the Na$_v$1.5 target. Through the oxygen substituents of the Amide group, compound **1c** forms a hydrogen bond with the Ca$_v$3.1 (6KZO) at the ASN 952 on the $S6_{II}$ helix and GLN 922 within the active site. Meanwhile, BIA 2-024 interacted with the carbonyl oxygen of LEU 353 with pi-sigma and pi-alkyl intermolecular forces. The result from Table 4 revealed from the molecular interaction of Acetazolamide with Ca$_v$3.1 that Acetazolamide is a potent Ca^{2+} inhibitor.

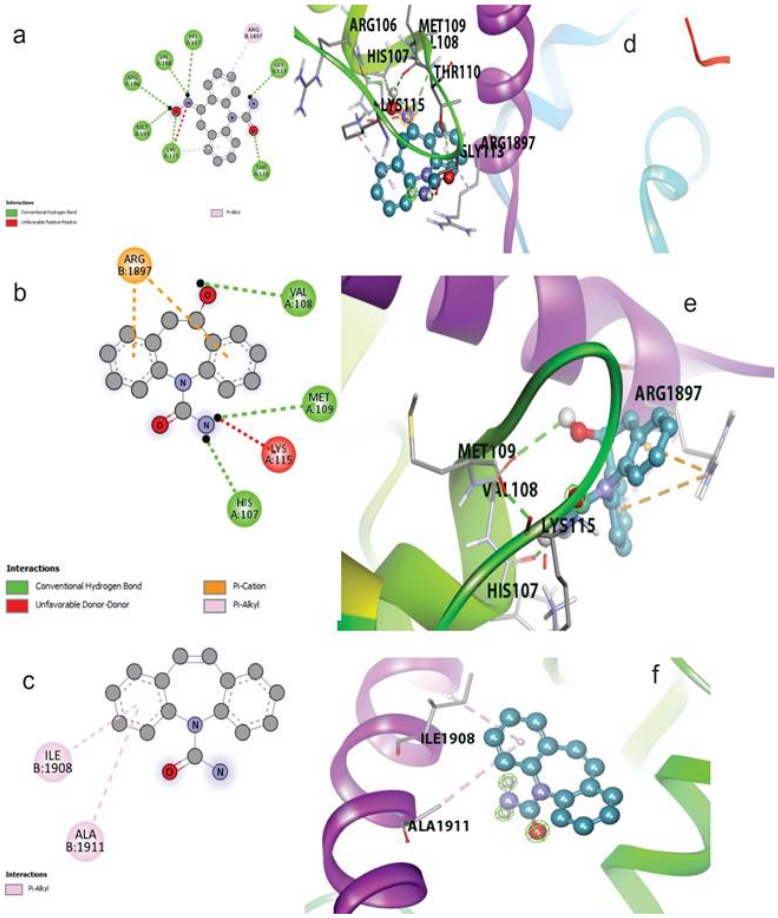

Figure 4. Graphical representation of the interaction of BIA 2-024 (2D, *a*, and 3D, *b*), Eslicarbazepine (2D, *b*, and 3D, *e*), and CBZ (2D, *c*, and 3D, *f*) at active binding site of Na$_v$1.5 (6MUD).

GABA (γ-amino butyric acid) is the most common inhibitory neurotransmitter in the CNS. A G-protein coupled receptor (GPCR) that causes slow and persistent synaptic inhibition is the metabotropic $GABA_B$ receptor. Presynaptic $GABA_B$ receptors inhibit neurotransmitter release, but postsynaptic $GABA_B$ receptors form a hyperpolarization of neurons. $GABA_B$ receptor dysfunction can result in a variety of neurological disorders, including pain, epilepsy,

and spasticity [48]. In this study, BIA 2-024 exhibits a stronger interfacial hydrogen bond interaction within the $GABA_B$ receptor subunit extracellular Venus Fly Trap ($GBR1b_{VFT}$) with SER 198. Accounting for the contribution of HCO_3^- current to the ionic current through γ-amino butyric acid ($GABA_B$) receptors on dendrites is increased during periods of high-frequency receptor activation. The excitatory effect of this HCO_3^- is blocked by membrane permeates carbonic anhydrase (CA) inhibitors [49]. However, BIA2-024 supersedes the others in considerable stability in the active site. The stabilization of the protein-ligand complex is mainly due to the H-bonds and hydrophobic interactions, which inhibit the receptor's activity.

Inhibiting the CA, hence increasing CO_2 levels in the brain, is one indirect method for treating epilepsy [50]. In mice, comparing the activity of acetazolamide (standard drug) with that of sulphanilamide using the maximum electroshock seizure (MES) test revealed a clear relationship between the anticonvulsant effect and inhibition of brain CA. The maximum degree of enzyme inhibition seen by these two drugs corresponded with their time of peak anticonvulsant effect, with acetazolamide predicted to be twice as powerful as sulphanilamide [51,52].

In addition to their anticonvulsant properties, the compounds showed high stability and molecular interactions with the hCA-II receptor. CBZ had the maximum binding affinity with the lowest energy of -8.4 kcal/mol with no bonding interaction with the receptor's residues (Table 3). Eslicarbazepine follows this with a binding energy of $-8.2\ kcal/mol$ located in the active site channel, where they are stabilized by the formation of hydrophobic interactions with the side chains of residues VAL121, VAL143, and LEU198. However, most of the compounds possess a good affinity than the standard drug for hCA-II. Carbamazepine, Eslicarbazepine, Oxcarbamazepine, BIA2-024, BIA2-093, R-LCM, 1a, 1b, and 1c are the compounds. In addition, 83 percent of the total compounds form one or more interaction(s) with the active site residues of hCA-II (see Table 3). This may indicate that most of the compounds are potent inhibitors of hCA-II. Moreover, one studied compound has recently entered phase I of clinical trials [53].

4. Conclusions

Understanding the molecular interactions of drugs that mediate epileptic seizures in the early stage of drug discovery can help in a more effective drug design. In this study, we employed *in silico* methods to validate prior findings from an experimental study of CBZ and R-LCM analogs. All analogs studied are chemically reactive, with Carbamazepine's analogs having the lowest band gap. The physicochemical parameters calculated using quantum mechanics showed that all the compounds are soft and have a high bioavailability. The pharmacokinetics properties of the compounds, through ADMET evaluation, confirm the potential drug-likeness properties of the compounds. These compounds in complex with four selected targets of epilepsy were studied at the molecular level using molecular docking studies by considering the binding affinity and the molecular interactions with the target's receptors. We selected those compounds that effectively cross the blood-brain barrier, have the appropriate physicochemical properties, are not rapidly metabolized, are non-toxic, and have high affinity and target selectivity (especially over $Ca_v3.1$ and $Na_v1.5$ channels). This result confirmed the inhibitory potency and selectivity for rapidly firing ("epileptic") neurons over neurons displaying normal activity of BIA 2-024, BIA 2-093, CBZ, and Eslicarbazepine. The result also ascertains the experimental result, which showed that the major mechanism of BIA 2-093 is the inhibition of voltage-dependent sodium channels and their safety in older patients.

The advantage of this protocol is the confirmation of the activity of these compounds in treating epilepsy. Some of the compounds described in this paper are suitable for clinical studies, and their evaluation is still ongoing, with great promise for developing novel drugs.

Funding

This research received no external funding.

Acknowledgments

The authors expressed their profound gratitude to the chemistry department at the University of Ibadan for access to the computational laboratory facilities. Conflicts of Interest
The authors declare no conflict of interest.

References

1. Eadie, M.J. Shortcomings in the current treatment of epilepsy. *Expert Rev. Neurother.* **2012**, *12*, 1419-1427, https://doi.org/10.1586/ern.12.129.
2. Holmes, G.L. Drug Treatment of Epilepsy Neuropsychiatric Comorbidities in Children. *Paediatr. Drugs* **2021**, *23*, 55-73, https://doi.org/10.1007/s40272-020-00428-w.
3. Jarvis, S.E.; Zamponi, G.W. Interactions between presynaptic Ca^{2+} channels, cytoplasmic messengers and proteins of the synaptic vesicle release complex. *Trends Pharmacol. Sci.* **2001**, *22*, 519-525, https://doi.org/10.1016/s0165-6147(00)01800-9.
4. Zamponi, G.W. Targeting voltage-gated calcium channels in neurological and psychiatric diseases. *Nat. Rev. Drug Discov.* **2016**, *15*, 19-34, https://doi.org/10.1038/nrd.2015.5.
5. Amaye, I.J.; Jackson-Ayotunde, P.L.; Martin-Caraballo, M. Evaluation of potential anticonvulsant fluorinated *N*-benzamide enaminones as *T*-type Ca^{2+} channel blockers. *Bioorg. Med. Chem.* **2022**, *65*, 116766, https://doi.org/10.1016/j.bmc.2022.116766.
6. Sack, A.-S.; Snutch, T.P. T-Type Calcium Channels in Epilepsy. In Voltage-Gated Calcium Channelsm, Zamponi, G.W., Weiss, N., Eds.; Springer, Cham, **2022**; 533-552, https://doi.org/10.1007/978-3-031-08881-0_20.
7. Dolphin, A.C. Voltage-gated calcium channels: Their discovery, function and importance as drug targets. *Brain Neurosci. Adv.* **2018**, *2*, 2398212818794805, https://doi.org/10.1177/2398212818794805.
8. Halling, D.B.; Aracena-Parks, P.; Hamilton, S.L. Regulation of Voltage-Gated Ca^{2+} Channels by Calmodulin. *Sci. STKE* **2005**, *2005*, re15, https://doi.org/10.1126/stke.3152005re15.
9. Organization, W.H. Epilepsy. Available online: https://www.who.int/news-room/fact-sheets/detail/epilepsy (accessed on 08-08-**2023**).
10. Wikipedia. Epilepsy, Wikipedia. **2017 (**Available online: (accessed on 08-08-2021).
11. Barker, B.S.; Ottolini, M.; Wagnon, J.L.; Hollander, R.M.; Meisler, M.H.; Patel, M.K. The *SCN8A* encephalopathy mutation p.Ile1327Val displays elevated sensitivity to the anticonvulsant phenytoin. *Epilepsia* **2016**, *57*, 1458-1466, https://doi.org/10.1111/epi.13461.
12. Alghamdi, M.A.; Al-Eitan, L.N.; Asiri, A.; Rababa'h, D.M.; Alqahtani, S.A.; Aldarami, M.S.; Alsaeedi, M.A.; Almuidh, R.S.; Alzahrani, A.A.; Sakah, A.H.; El Nashar, E.M.; Otaif, M.Y.; Abdel Ghaffar, N.F. Association of sodium voltage-gated channel genes polymorphisms with epilepsy risk and prognosis in the Saudi population. *Ann. Med.* **2022**, *54*, 1938-1951, https://doi.org/10.1080/07853890.2022.2096257.
13. Zhang, S.; Zhu, Y.; Cheng, J.; Tao, J. Ion Channels in Epilepsy: Blasting Fuse for Neuronal Hyperexcitability. In Epilepsy - Advances in Diagnosis and Therapy, Al-Zwaini, I.J., Albadri, B.A.-H.M., Eds.; IntechOpen, **2019**; 1-12, https://doi.org/10.5772/intechopen.83698.
14. Dyong, T.M.; Gess, B.; Dumke, C.; Rolke, R.; Dohrn, M.F. Carbamazepine for Chronic Muscle Pain: A Retrospective Assessment of Indications, Side Effects, and Treatment Response. *Brain Sci.* **2023**, *13*, 123, https://doi.org/10.3390/brainsci13010123.
15. Ghosh, N.; Mondal, S.; Chakraborty, S.; Ghosh, M. A Stability Indicating Method was Developed and Validation for the Estimation of Carbamazepine in Bulk and Tablet Dosage form by UV-Spectroscopic Techniques. *J. Drug Deliv. Ther.* **2023**, *13*, 85-104, https://doi.org/10.22270/jddt.v13i3.5987.

16. Veggiotti, P.; Józwiak, S.; Kirkham, F.; Moreira, J.; Pereira, A.; Ikedo, F.; Gama, H. Long-term therapeutic effect of eslicarbazepine acetate in children: An open-label extension of a cognition study in children aged 6–16 years. *Epilepsy Behav.* **2022**, *127*, 108515, https://doi.org/10.1016/j.yebeh.2021.108515.
17. Zavala-Tecuapetla, C.; Manjarrez-Marmolejo, J.; Ramírez-Jarquín, J.O.; Rivera-Cerecedo, C.V. Eslicarbazepine, but Not Lamotrigine or Ranolazine, Shows Anticonvulsant Efficacy in Carbamazepine-Resistant Rats Developed by Window-Pentylenetetrazole Kindling. *Brain Sci.* **2022**, *12*, 629, https://doi.org/10.3390/brainsci12050629.
18. Wang, Y.; Brittain, J.M.; Jarecki, B.W.; Park, K.D.; Wilson, S.M.; Wang, B.; Hale, R.; Meroueh, S.O.; Cummins, T.R.; Khanna, R. *In Silico* Docking and Electrophysiological Characterization of Lacosamide Binding Sites on Collapsin Response Mediator Protein-2 Identifies a Pocket Important in Modulating Sodium Channel Slow Inactivation. *J. Biol. Chem.* **2010**, *285*, 25296-25307, https://doi.org/10.1074/jbc.M110.128801.
19. Gutiérrez-Álvarez, A.M.; Sagarra-Mur, D.; Jiménez-Corral, C. Lacosamida, nuevo antiepiléptico con amplias perspectivas. [Lacosamide, new antiepileptic with broad perspectives]. *Neurología* **2011**, *26*, 568-569, https://doi.org/10.1016/j.nrl.2011.03.002.
20. Ishikawa, N.; Eguchi, Y.; Izumo, H.; Tateishi, Y.; Tani, H.; Kobayashi, Y.; Okada, S. Clinical impact of the dose and blood concentration of lacosamide in Japanese pediatric patients with epilepsy: A cohort study. *Epilepsy Behav.* **2022**, *129*, 108614, https://doi.org/10.1016/j.yebeh.2022.108614.
21. Mo, F.; Meletti, S.; Belcastro, V.; Quadri, S.; Napolitano, M.; Bello, L.; Dainese, F.; Scarpelli, M.; Florindo, I.; Mascia, A.; Pauletto, G.; Bruno, F.; Pellerino, A.; Giovannini, G.; Polosa, M.; Sessa, M.; Conti Nibali, M.; Di Gennaro, G.; Gigli, G.L.; Pisanello, A.; Cavallieri, F.; Rudà, R. Lacosamide in monotherapy in BTRE (brain tumor-related epilepsy): results from an Italian multicenter retrospective study. *J. Neurooncol.* **2022**, *157*, 551-559, https://doi.org/10.1007/s11060-022-03998-6.
22. Çarçak, N.; Karanfil, C.; Akat, Ş.; Akman, Ö.; Onat, F. The effect of chronic treatment with sodium channel blocker lacosamide on early development of absence seizures in genetic absence epilepsy rats. *Epilepsy Res.* **2022**, *182*, 106896, https://doi.org/10.1016/j.eplepsyres.2022.106896.
23. Jeong, H.; Yadav, N.N.; Ha, H.-J. Synthesis of Lacosamide (Vimpat) and Its Derivatives from Aziridine-(2*R*)-carboxylate. *Synthesis* **2017**, *49*, 1264-1272, https://doi.org/10.1055/s-0036-1588093.
24. Moutal, A.; François-Moutal, L.; Perez-Miller, S.; Cottier, K.; Chew, L.A.; Yeon, S.K.; Dai, J.; Park, K.D.; Khanna, M.; Khanna, R. (S)-Lacosamide Binding to Collapsin Response Mediator Protein 2 (CRMP2) Regulates CaV2.2 Activity by Subverting Its Phosphorylation by Cdk5. *Mol. Neurobiol.* **2016**, *53*, 1959-1976, https://doi.org/10.1007/s12035-015-9141-2.
25. Bank, P.D. RCSB PDB: Homepage. Available online: (accessed on 10-30-2021).
26. Geng, Y.; Bush, M.; Mosyak, L.; Wang, F.; Fan, Q.R. Structural mechanism of ligand activation in human $GABA_B$ receptor. *Nature* **2013**, *504*, 254-259, https://doi.org/10.1038/nature12725.Structural.
27. Zhao, Y.; Huang, G.; Wu, Q.; Wu, K.; Li, R.; Lei, J.; Pan, X.; Yan, N. Cryo-EM structures of apo and antagonist-bound human $Ca_v3.1$. *Nature* **2019**, *576*, 492-497, https://doi.org/10.1038/s41586-019-1801-3.
28. Gabelli, S.B.; Boto, A.; Kuhns, V.H.; Bianchet, M.A.; Farinelli, F.; Aripirala, S.; Yoder, J.; Jakoncic, J.; Tomaselli, G.F.; Amzel, L.M. Regulation of the $Na_V1.5$ cytoplasmic domain by calmodulin. *Nat. Commun.* **2014**, *5*, 5126, https://doi.org/10.1038/ncomms6126.
29. Gardill, B.R.; Rivera-Acevedo, R.E.; Tung, C.-C.; Van Petegem, F. Crystal structures of Ca^{2+}-calmodulin bound to Na_V C-terminal regions suggest role for EF-hand domain in binding and inactivation. *Proc. Natl. Acad. Sci. USA* **2019**, *116*, 10763-10772, https://doi.org/10.1073/pnas.1818618116.
30. Di Fiore, A.; De Simone, G.; Alterio, V.; Riccio, V.; Winum, J.-Y.; Carta, F.; Supuran, C.T. The anticonvulsant sulfamide JNJ-26990990 and its *S*,*S*-dioxide analog strongly inhibit carbonic anhydrases: solution and X-ray crystallographic studies. *Org. Biomol. Chem.* **2016**, *14*, 4853-4858, https://doi.org/10.1039/c6ob00803h.
31. Tian, W.; Chen, C.; Lei, X.; Zhao, J.; Liang, J. CASTp 3.0: computed atlas of surface topography of proteins. *Nucleic Acids Res.* **2018**, *46*, W363-W367, https://doi.org/10.1093/nar/gky473.
32. Ambrósio, A.F.; Soares-da-Silva, P.; Carvalho, C.M.; Carvalho, A.P. Mechanisms of Action of Carbamazepine and Its Derivatives, Oxcarbazepine, BIA 2-093, and BIA 2-024. *Neurochem. Res.* **2002**, *27*, 121-130, https://doi.org/10.1023/a:1014814924965.
33. Becke, A.D. Density-functional thermochemistry. III. The role of exact exchange. *J. Chem. Phys.* **1993**, *98*, 5648-5652, https://doi.org/10.1063/1.464913.

34. Stephens, P.J.; Devlin, F.J.; Chabalowski, C.F.; Frisch, M.J. Ab Initio Calculation of Vibrational Absorption and Circular Dichroism Spectra Using Density Functional Force Fields. *J. Phys. Chem.* **1994**, *98*, 11623-11627, https://doi.org/10.1021/j100096a001.
35. Molsoft. Molsoft L.L.C.: Drug-Likeness and molecular property prediction. Available online: https://www.molsoft.com/mprop/ (accessed on 09-16-**2021**).
36. Lipinski, C.A.; Lombardo, F.; Dominy, B.W.; Feeney, P.J. Experimental and computational approaches to estimate solubility and permeability in drug discovery and development settings. *Adv. Drug Deliv. Rev.* **2012**, *64*, 4-17, https://doi.org/10.1016/j.addr.2012.09.019.
37. Yang, H.; Lou, C.; Sun, L.; Li, J.; Cai, Y.; Wang, Z.; Li, W.; Liu, G.; Tang, Y. admetSAR 2.0: web-service for prediction and optimization of chemical ADMET properties. *Bioinformatics* **2019**, *35*, 1067-1069, https://doi.org/10.1093/bioinformatics/bty707.
38. Adejoro, I.A.; Babatunde, D.D.; Tolufashe, G.F. Molecular docking and dynamic simulations of some medicinal plants compounds against SARS-CoV-2: an *in silico* study. *J. Taibah Univ. Sci.* **2020**, *14*, 1563-1570, https://doi.org/10.1080/16583655.2020.1848049.
39. Dallakyan, S.; Olson, A.J. Small-Molecule Library Screening by Docking with PyRx. In Chemical Biology. Methods in Molecular Biology, Hempel, J., Williams, C., Hong, C., Eds.; Humana Press, New York, NY, **2015**; Volume 1263, 243-250, https://doi.org/10.1007/978-1-4939-2269-7_19.
40. Kaya, S.; Kaya, C. A new equation for calculation of chemical hardness of groups and molecules. *Mol. Phys.* **2015**, *113*, 1311-1319, https://doi.org/10.1080/00268976.2014.991771.
41. Pérez, P.; Domingo, L.R.; Aizman, A.; Contreras, R. Chapter 9 The electrophilicity index in organic chemistry. In Theoretical and Computational Chemistry, Toro-Labbé, A., Ed.; Elsevier, **2007**; Volume 19, 139-201, https://doi.org/10.1016/S1380-7323(07)80010-0.
42. Umar, U. Computational Study of Anticorrosive Effects of Some Thiazole Derivatives Against the Corrosion of Aluminium. *Rhazes: Green Appl. Chem.* **2020**, *10*, 113-128, https://doi.org/10.48419/IMIST.PRSM/rhazes-v10.23814.
43. Elekofehinti, O.O.; Iwaloye, O.; Josiah, S.S.; Lawal, A.O.; Akinjiyan, M.O.; Ariyo, E.O. Molecular docking studies, molecular dynamics and ADME/tox reveal therapeutic potentials of STOCK1N-69160 against papain-like protease of SARS-CoV-2. *Mol. Divers.* **2021**, *25*, 1761-1773, https://doi.org/10.1007/s11030-020-10151-w.
44. Hassan, A.U.; Li, Y. Convenient and facile theoretical design strategy to amplify NLO response of N-doped-indolo[3,2,1-jk]carbazole *push–pull* A-π-D-π-A switches. *J. Chem. Technol. Biotechnol.* **2024**, *99*, 355-369, https://doi.org/10.1002/jctb.7530.
45. Alavijeh, M.S.; Chishty, M.; Qaiser, M.Z.; Palmer, A.M. Drug metabolism and pharmacokinetics, the blood-brain barrier, and central nervous system drug discovery. *NeuroRx* **2005**, *2*, 554-571, https://doi.org/10.1602/neurorx.2.4.554.
46. Gosselet, F.; Loiola, R.A.; Roig, A.; Rosell, A.; Culot, M. Central nervous system delivery of molecules across the blood-brain barrier. *Neurochem. Int.* **2021**, *144*, 104952, https://doi.org/10.1016/j.neuint.2020.104952.
47. Adelusi, T.I.; Oyedele, A.-Q.K.; Boyenle, I.D.; Ogunlana, A.T.; Adeyemi, R.O.; Ukachi, C.D.; Idris, M.O.; Olaoba, O.T.; Adedotun, I.O.; Kolawole, O.E.; Xiaoxing, Y.; Abdul-Hammed, M. Molecular modeling in drug discovery. *Inform. Med. Unlocked.* **2022**, *29*, 100880, https://doi.org/10.1016/j.imu.2022.100880.
48. Villemure, E.; Volgraf, M.; Jiang, Y.; Wu, G.; Ly, C.Q.; Yuen, P.-w.; Lu, A.; Luo, X.; Liu, M.; Zhang, S.; Lupardus, P.J.; Wallweber, H.J.A.; Liederer, B.M.; Deshmukh, G.; Plise, E.; Tay, S.; Wang, T.-M.; Hanson, J.E.; Hackos, D.H.; Scearce-Levie, K.; Schwarz, J.B.; Sellers, B.D. GluN2A-Selective Pyridopyrimidinone Series of NMDAR Positive Allosteric Modulators with an Improved in Vivo Profile. *ACS Med. Chem. Lett.* **2017**, *8*, 84-89, https://doi.org/10.1021/acsmedchemlett.6b00388.
49. Sethi, K.K.; Nayak, P.K.; Sarkar, H.; Verma, S.M. A Rational Approach towards the Development of Human Carbonic Anhydrase Inhibitors as Antiepileptic Agent. *Med. Chem.* **2016**, *6*, 405-410, https://doi.org/10.4172/2161-0444.1000377.
50. Aggarwal, M.; Kondeti, B.; McKenna, R. Anticonvulsant/antiepileptic carbonic anhydrase inhibitors: a patent review. *Expert Opin. Ther. Pat.* **2013**, *23*, 717-724, https://doi.org/10.1517/13543776.2013.782394.
51. Millichap, J.G.; Woodbury, D.M.; Goodman, L.S. Mechanism of the anticonvulsant action of acetazoleamide, a carbonic anhydrase inhibitor. *J. Pharmacol. Exp. Ther.* **1955**, *115*, 251-258.
52. Rankin, G.O. Acetazolamide. In xPharm: The Comprehensive Pharmacology Reference, Enna, S.J., Bylund, D.B., Eds.; Elsevier, New York, **2023**; 1-5, https://doi.org/10.1016/B978-008055232-3.61158-4.

53. Andermann, E.; Rosenfeld, W.; Penovich, P.; Rogin, J.; Cendes, F.; Carreño, M.; Ramsay, R.E.; Ben-Menachem, E.; Gama, H.; Rocha, F.; Soares-da-Silva, P.; Tosiello, R.; Blum, D.; Grinnell, T. Comparative analysis of the safety and tolerability of eslicarbazepine acetate in older (≥60 years) and younger (18–59 years) adults. *Epilepsy Res.* **2021**, *169*, 106478, https://doi.org/10.1016/j.eplepsyres.2020.106478.